

## Liquid–Liquid Miscibility Gaps in Drug–Water Binary Systems: Crystal Structure and Thermodynamic Properties of Prilocaine and the Temperature–Composition Phase Diagram of the Prilocaine–Water System

Ivo B. Rietveld,<sup>\*,†</sup> Marc-Antoine Perrin,<sup>‡</sup> Siro Toscani,<sup>§</sup> Maria Barrio,<sup>||</sup> Beatrice Nicolai,<sup>†</sup> Josep-Lluis Tamarit,<sup>||</sup> and René Ceolin<sup>†,||</sup>

<sup>†</sup>EAD Physico-chimie Industrielle du Médicament (EA 4066), Faculté de Pharmacie, Université Paris Descartes, 4, Avenue de l'Observatoire, 75006 Paris, France

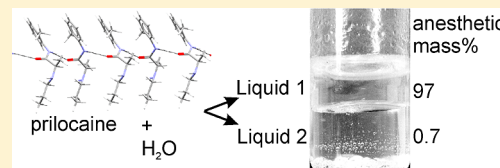
<sup>‡</sup>Sanofi R&D, Lead Generation & Compound Realization/Analytical Sciences/Solid State group, 13, Quai Jules Guesde, 94400 Vitry sur Seine, France

<sup>§</sup>Département de Chimie—UMR 6226, Faculté des Sciences, Université de Rennes 1, Bâtiment 10B, 263, Avenue du Général Leclerc, 35042 Rennes Cedex, France

<sup>||</sup>Grup de Caracterització de Materials (GCM), Departament de Física i Enginyeria Nuclear, Universitat Politècnica de Catalunya, ETSEIB, Diagonal 647, 08028 Barcelona, Spain

**ABSTRACT:** EMLA cream, a “eutectic mixture of local anesthetics”, was developed in the early 1980s by Astra Pharmaceutical Production. The mixture of anesthetics containing lidocaine, prilocaine, and water is liquid at room temperature, which is partly due to the eutectic equilibrium between prilocaine and lidocaine at 293 K, as was clear from the start. However, the full thermodynamic background for the stability of the liquid and its emulsion-like appearance has never been elucidated. In the present study of the binary system prilocaine–water, a region of liquid–liquid demixing has been observed, linked to a monotectic equilibrium at 302.4 K. It results in a prilocaine-rich liquid containing approximately 0.7 mol fraction of anesthetic. Similar behavior has been reported for the binary system lidocaine–water (Ceolin, R.; et al. *J. Pharm. Sci.* **2010**, *99* (6), 2756–2765). In the ternary mixture, the combination of the monotectic equilibrium and the above-mentioned eutectic equilibrium between prilocaine and lidocaine results in an anesthetic-rich liquid that remains stable below room temperature. This liquid forms an emulsion-like mixture in the presence of an aqueous solution saturated with anesthetics. Physical properties and the crystal structure of prilocaine are also reported.

**KEYWORDS:** crystal structure, thermodynamics, phase behavior, local anesthetic, EMLA cream, physical properties



### 1. INTRODUCTION

EMLA cream (EMLA stands for “eutectic mixture of local anesthetics”) was developed in the early 1980s by Astra Pharmaceutical Production AB, Sweden, presently known by the name AstraZeneca.<sup>1–3</sup> The cream is described as a “nonconventional emulsion” based on a eutectic mixture of lidocaine and prilocaine with a 1:1 molar ratio. The addition of water leads to a “melting” temperature below room temperature; therefore, under ambient conditions, the mixture is an oily “emulsion system [that] does not contain any lipophilic solvent”.<sup>3</sup> However, what is the cause behind the stability of the emulsion? In the absence of any stabilizing agents, the stability must be caused by the inherent thermodynamics of the system. A first clue to the answer is given by the behavior of the lidocaine–water system, which has been described recently.<sup>4</sup> It was found that a liquid–liquid miscibility gap, i.e., an invariant equilibrium involving a water-rich liquid and a lidocaine-rich liquid, forms at 321 K. A miscibility gap occurs if the interaction enthalpy between two different molecules (A and B) in the

liquid state is less favorable than the interaction enthalpy between molecules of the same kind (A–A and B–B). Miscibility gaps provide access to liquids much richer in active pharmaceutical ingredients (APIs) than saturated aqueous solutions. Using miscibility gaps to increase drug content in solutions has been suggested previously in reports on other drug–water systems (barbital and phenobarbital).<sup>5,6</sup> Nonetheless, the miscibility gap in the lidocaine–water system can only be part of the answer to the stability of the stable emulsion, because the monotectic equilibrium is found at 321 K, well above room temperature and above the temperature of the human epidermis.

The prilocaine–water system has been investigated as the third part of the ternary system lidocaine–prilocaine–water

**Received:** September 24, 2012

**Revised:** December 17, 2012

**Accepted:** January 21, 2013

**Published:** January 22, 2013

constituting the main EMLA ingredients. In the process, the crystal structure of prilocaine has been solved. This paper consists, therefore, of two parts: the first reports on the crystal structure of prilocaine and its main thermodynamic properties (see Figure 1 for the chemical structure of prilocaine). The

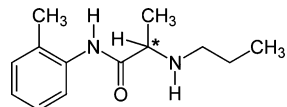


Figure 1. Chemical structure of prilocaine.

second part reports on the temperature–composition phase diagram of the prilocaine–water system and discusses its phase behavior in relation to the lidocaine–water system and the EMLA mixture.

## 2. EXPERIMENTAL SECTION

Prilocaine of medicinal grade had been provided by former Roger Bellon laboratory (now Sanofi, France) and had been left at room temperature since 1988 in a sealed brown flask protected from light. Prilocaine (*N*-(2-methylphenyl)-2-(propylamino)propanamide,  $C_{13}H_{20}N_2O$ ,  $M = 220.31$ ) contains an asymmetric carbon atom (see Figure 1); however, no information had been provided as to whether the sample was a racemic mixture of enantiomers (conglomerate), a racemic compound (true racemate), or even either one of the pure enantiomers. A second batch of (RS)-prilocaine was purchased from SIGMA France for verification of the thermal analysis and density measurements obtained with the 20-year-old batch.

**2.1. High-Resolution X-ray Powder Diffraction (XRPD) as a Function of Temperature.** XRPD measurements using the Debye–Scherrer geometry and transmission mode were carried out with a vertically mounted INEL cylindrical position-sensitive detector (CPS-120).<sup>7</sup> Monochromatic Cu  $K\alpha_1$  ( $\lambda = 1.54056 \text{ \AA}$ ) radiation was selected by an asymmetrically focusing incident-beam curved quartz monochromator. Low-temperature measurements were carried out with a liquid nitrogen 700 series Cryostream Cooler from Oxford Cryosystems. Cubic phase  $Na_2Ca_3Al_2F_4$  was used for external calibration.<sup>8</sup> The PEAKOC application from the DIFFRACT-INEL program was used for calibration as well as for the determination of the peak positions. After indexing, lattice parameters were refined by least-squares minimization with the FullProf suite.<sup>9</sup>

The specimen rotated perpendicularly to the X-ray beam during the experiments to improve the averaging over the crystallite orientations. Before each isothermal data acquisition, the specimen was allowed to equilibrate for approximately 10 min, and each acquisition time was no less than 1 h. The heating rate in between data collection was  $1.33 \text{ K min}^{-1}$ . Patterns were recorded on heating in the temperature range from 100 K up to the melting point.

**2.2. Crystal Structure Determination from High-Resolution X-ray Powder Diffraction Data at Room Temperature.** A sample was introduced in a Lindemann capillary (0.5 mm diameter) and analyzed at room temperature on a high angular resolution X-ray diffractometer (PANalytical X'Pert Pro MPD, Debye–Scherrer transmission geometry, equipped with a hybrid monochromator offering a parallel beam of pure Cu  $K\alpha_1$  radiation). The obtained powder pattern was used for indexing. Taking 20 positions of well separated

single peaks, the X-CELL indexing program<sup>10</sup> found a monoclinic unit cell and suggested the space group  $P2_1/c$ , based on systematic absences. This assignment was confirmed by a modified Pawley refinement.<sup>11</sup>

Based on the molecular geometry obtained from lidocaine single-crystal XRD data<sup>12</sup> the prilocaine molecular model was sketched using Material Studio software (Accelrys, Inc., 2003 San Diego). Trial crystal structures were generated by stochastic movements of the prilocaine molecule within the previously indexed crystal cell.<sup>11</sup> Intermolecular torsion angles were allowed to vary in combination with different orientations and positions of the molecule within the asymmetric unit. For each trial structure, a powder pattern was simulated and compared to the experimental data. The acceptance criterion for each successive structural model was a lower  $R_{wp}$  profile factor. An acceptance probability was used for trial structures with an unfavorable  $R_{wp}$  profile factor. Finally, to optimize the crystal structure with the lowest  $R_{wp}$ , Rietveld refinement was used.

For the Rietveld refinement, data out to  $60^\circ 2\theta$  were used, which corresponds to  $1.54 \text{ \AA}$  real-space resolution. The Rietveld refinement was carried out with TOPAS-Academic.<sup>13</sup> Restraints were included for all bond lengths and bond angles and for the planarity of the aromatic ring; the values for the restraints were taken from the DFT-D calculations (see below). A global  $B_{iso}$  was refined for all non-hydrogen atoms, with the  $B_{iso}$  of the hydrogen atoms constrained at 1.2 times the value of the global  $B_{iso}$ . The inclusion of a preferred-orientation correction with the March–Dollase formula<sup>14</sup> was tried for directions (100), (010), and (001). The preferred-orientation correction for the (100) and (001) directions made a significant difference to the  $R_{wp}$  value, with opposite deviations of the March–Dollase parameter from 1. The directions (−101), (−102), and (−103) were tried, with (−102) giving slightly better results, and it was this direction that was used.

The molecular geometry was checked with Mogul,<sup>15</sup> which compares each bond length and bond angle to corresponding distributions from single-crystal data.

**2.3. Proof of Structure Using Density Functional Theory (DFT) Calculations.** The crystal structure determined from powder data was energy-optimized with the program GRACE,<sup>16</sup> which uses VASP<sup>17–19</sup> for single-point pure density functional theory (DFT) calculations. The generalized gradient approximation (GGA) with the Perdew–Wang 91<sup>20</sup> exchange-correlation functional was used, with standard projector-augmented wave (PAW) potentials. The plane-wave cutoff energy was 520 eV, and the  $k$ -point spacing was approximately  $0.7 \text{ \AA}^{-1}$ . The DFT calculations were augmented with a dispersion correction to give a dispersion-corrected DFT potential, or DFT-D potential. The settings for the DFT calculations as well as a full description of the dispersion correction are given in Neumann and Perrin.<sup>21</sup> The root mean square (RMS) Cartesian displacement of the non-hydrogen atoms of the energy-minimized crystal structure with respect to the experimental structure was calculated as described in ref 22.<sup>22–24</sup> From calculations on a validation set of 225 organic single-crystal structures, it is known that RMS Cartesian displacement values up to  $0.25 \text{ \AA}$  indicate that the structure is correct, whereas values greater than  $0.30 \text{ \AA}$  point to an incorrect structure.

Hydrogen atoms are poor X-ray scatterers, and their positions cannot be determined reliably from X-ray powder diffraction data. Usually, all hydrogen atoms can be located

based on chemical considerations, but in the structure of prilocaine, the position of one of the two N–H hydrogen atoms is ambiguous. Assigning a position to the N–H hydrogen atom in the amide group is trivial: it must lie in the plane of the amide group because the nitrogen atom is  $sp^2$  hybridized and because otherwise no hydrogen bond can be formed. The second N–H hydrogen atom, however, has two possible positions, because the second nitrogen is  $sp^3$  hybridized. Both positions were tried, and for both possibilities a DFT-D calculation was run with variable lattice parameters with the experimental space-group symmetry imposed.

**2.4. Differential Scanning Calorimetry.** Calorimetric data were obtained with a Q100 thermal analyzer from TA Instruments with heating rates of 5 and 10  $K \cdot min^{-1}$ . The analyzer was calibrated with indium ( $T_{fus} = 429.75\text{ K}$  and  $\Delta_{fus}H = 3.267\text{ kJ mol}^{-1}$ ). Prilocaine was weighed using a microbalance sensitive to 0.01 mg and sealed in aluminum pans.

**2.5. High-Pressure Differential Thermal Analysis.** HP-DTA measurements were carried out at a  $2\text{ K min}^{-1}$  heating rate using an in-house built high-pressure differential thermal analyzer similar to Würflinger's apparatus<sup>25</sup> that operates between 298 and 473 K and 0 and 250 MPa. To ascertain that in-pan volumes were free from residual air, specimens were mixed with an inert perfluorinated liquid (Galden, from Bioblock Scientifics, Illkirch, France) as a pressure-transmitting medium, and the mixtures were sealed into cylindrical tin pans. To verify that the perfluorinated liquid was chemically inactive and that it would not affect the melting temperature of prilocaine, DSC measurements were carried out on a Galden–prilocaine mixture with the TA Instruments Q100 under ordinary conditions.

**2.6. Liquid Density Measurements as a Function of Temperature.** Liquid density as a function of temperature was determined with a DMA-5000 density meter from Anton-Paar. Data were obtained at isothermal intervals while slowly and stepwise cooling from 360 to 300 K. Dry air and bidistilled water were used as calibration standards in the temperature range. Once the temperature inside the apparatus had equilibrated above the temperature of fusion, the specimen was introduced with an in-house built filling device. The temperature was controlled with a precision of  $\pm 1\text{ mK}$ .

### 3. RESULTS

**3.1. Crystal Structure of Racemic Prilocaine.** Single crystals of prilocaine had spontaneously grown by sublimation-condensation in its container over a 20 year period. The crystals consisted of thin needles (Figure 2) too thin for single crystal X-ray diffraction structure determination; therefore, the needles were analyzed by high-resolution X-ray powder diffraction.

The Rietveld refinement progressed smoothly and produced a good fit with  $\chi^2 = 1.273$ ,  $R'_{p} = 9.420$ , and  $R'_{wp} = 8.388$  (values after background correction) and  $R_p = 2.650$  and  $R_{wp} = 3.406$  (values before background subtraction). The March–Dollase parameter<sup>14</sup> for the (−102) direction refined to a value of 0.968(2);  $B_{iso}$  refined to 2.78(13)  $\text{\AA}^2$ . The resulting fit of the powder diffraction pattern can be found in Figure 3, and the crystal structure and refinement data can be found in Table 1.

As mentioned in the Experimental Section, the position of an N–H hydrogen atom was ambiguous. Two models were prepared, in which the hydrogen atom was manually placed in one of the two possible positions. The two models were energy-minimized with the DFT-D method, and then the RMSD value of each model was calculated. The energy

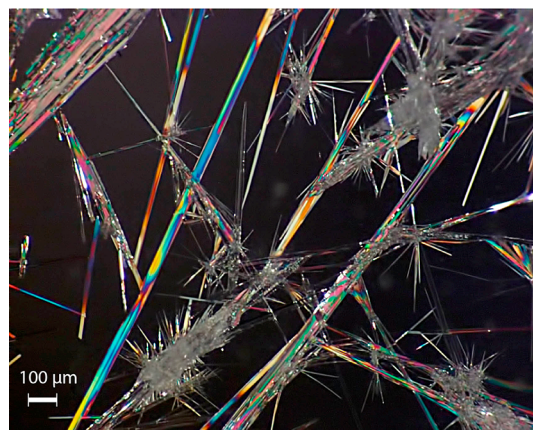


**Figure 2.** Crystal needles as obtained from the sample container by sublimation-condensation over 20 years.

minimizations took 12 h each on four 1 GHz 64-bit quad-core Opteron processors. For one of the models, the RMSD value was 0.42  $\text{\AA}$ , a strong indication that the structure is incorrect. The lattice energy for the other crystal structure was 4.8 kcal  $\text{mol}^{-1}$  more favorable, and the RMS Cartesian displacement was only 0.11  $\text{\AA}$ . This proves beyond reasonable doubt that this is the correct position for the N–H hydrogen; moreover, this is a strong indication that the crystal structure as a whole is correct. All results given in this paper refer to the structure with the latter position for the N–H hydrogen atom, which from here on is considered as the correct position.

According to the geometry check with *Mogul* of the crystal structure of prilocaine from powder diffraction data, all bond lengths are within at most 0.78 standard deviation from their mean single-crystal values and all bond angles are within at most 2.06 standard deviations from their mean single-crystal values. It can be concluded that the crystals are a racemic compound with both (R)- and (S)-prilocaine forming part of the structure. The molecular structure can be seen in Figure 4. Supplementary crystallographic data can be found in the CCDC, deposit number 902387, and obtained free of charge from the Cambridge Crystallographic Data Centre via [www.ccdc.cam.ac.uk/data\\_request/cif/](http://www.ccdc.cam.ac.uk/data_request/cif/).

The racemic crystal of (RS)-prilocaine contains an infinite hydrogen chain interconnecting alternately (R)- and (S)-prilocaine as can be seen in Figure 5. This chain runs along the *c* axis of the unit cell and is made up of hydrogen bonds with a donor–acceptor distance of 3.025  $\text{\AA}$ . A much weaker hydrogen bond (Figure 5c) can be found running along the *b* axis between the amine group with the hydrogen atom placed by the DFT calculations and the oxygen of the amide group with a donor–acceptor distance of 3.404  $\text{\AA}$ . The corresponding molecule reciprocates this hydrogen bond with its own amine group; thus, each pair of (R)- and (S)-prilocaine molecules is interconnected by two weak hydrogen bonds. In the direction of the *a* axis the interactions are mainly van der Waals in nature.

Both the aromatic rings as well as the aliphatic chains of the prilocaine molecules are aligned in their respective planes that run along the *b* axis. The angle between the two planes is approximately 49°.

**3.2. Calorimetric Data for Racemic Prilocaine.** The temperature of fusion of (RS)-prilocaine has been determined by DSC (onset value) and was found to be  $T_{fus} = 311.5 \pm 1.0\text{ K}$ . The specific enthalpy of melting is  $\Delta_{fus}h = 147 \pm 5\text{ J g}^{-1}$  (32.4  $\text{kJ mol}^{-1}$ ). The temperature and enthalpy of melting had

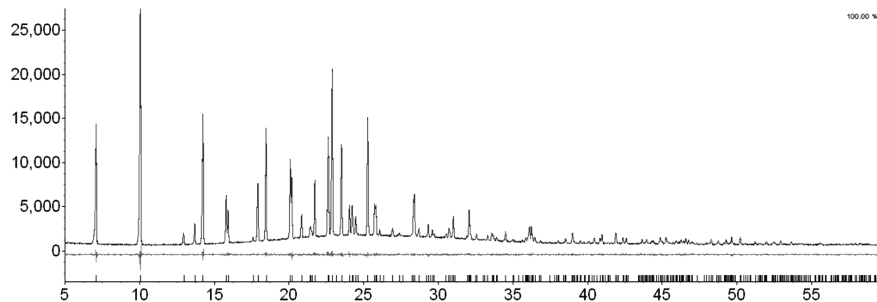


**Figure 3.** Powder diffraction pattern of prilocaine with Rietveld refinement and underneath the difference curve.

**Table 1. Crystal Data and Structure Refinement of Prilocaine**

*Crystal Data*

$C_{13}H_{20}ON_2$

$M_r = 220.31$

monoclinic,  $P2_1/c$

$a = 12.68570(16)$  Å

$b = 12.42470(16)$  Å

$c = 8.33776(7)$  Å

$\beta = 101.5266(6)^\circ$

$V = 1287.66(3)$  Å $^3$

$Z = 4$

$D_x = 1.136$  g cm $^{-3}$

Cu  $K\alpha_1$  radiation

$\mu = 0.095$  mm $^{-1}$

$T = 293$  K

specimen shape: cylinder 10 × 0.5 mm

*Data Collection*

diffractometer: Panalytical X'pert pro MRD

specimen mounting: Lindemann glass capillary 0.5 mm

specimen mounted in transmission mode

detector: X'celerator (Real Time Multiple Strip)

absorption correction: none

$2\theta_{\min} = 5.0^\circ$ ,  $2\theta_{\max} = 60.0^\circ$

increment in  $2\theta = 0.0167^\circ$

*Refinement*

refinement on  $I_{\text{net}}$

$R_{wp} = 3.406$

$R_p = 2.650$

$R_{\text{exp}} = 2.676$

$\chi^2 = 1.273$

profile function: modified Thompson–Cox–Hastings pseudo-Voigt

379 reflections

159 parameters

100 restraints

H-atom parameters restrained

weighting scheme based on measured s.u.'s  $w = 1/\sigma(Y_{\text{obs}})^2$

$(\Delta/\sigma)_{\text{max}} = 0.001$

preferred orientation correction: March–Dollase with direction  $(-102)$  and a March–Dollase parameter of 0.968(2)

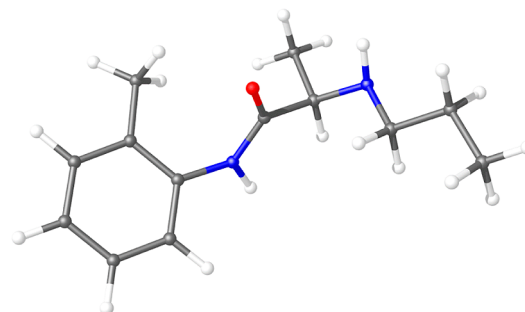


**Figure 4.** Molecular structure of prilocaine as determined by X-ray diffraction.

increase linearly as the temperature increases, and it was fitted to ( $r^2 = 0.9999$ )

$$v_L/(\text{cm}^3 \text{ g}^{-1}) = 7.66(3) \times 10^{-4}T/\text{K} + 0.7610(9) \quad (1)$$

X-ray powder diffraction as a function of temperature resulted in the following equation for the specific volume of solid prilocaine ( $r^2 = 0.9998$ ):

$$\begin{aligned} v_S/(\text{cm}^3 \text{ g}^{-1}) = & 3.26(20) \times 10^{-7}T^2/\text{K}^2 + 4.56(81) \\ & \times 10^{-5}T/\text{K} + 0.8379(8) \end{aligned} \quad (2)$$

At fusion, 311.5 K, the specific volume of solid racemic prilocaine equals  $0.884 \pm 0.001$  cm $^3$  g $^{-1}$  and the specific volume of the melt is  $1.000 \pm 0.002$  cm $^3$  g $^{-1}$ . These two values lead to a volume change on melting of  $\Delta_{\text{fus}}v = 0.116 \pm 0.003$  cm $^3$  g $^{-1}$ .

Extrapolating the thermal expansion of the liquid to low temperature, the specific volume of the liquid will cross the specific volume of the solid at the so-called Kauzmann temperature; for the present system that happens at 112 K. Here, the specific volume of the liquid becomes smaller than that of the solid. This is impossible considering that the liquid is a disordered system, and it is known as the Kauzmann paradox. However, generally well above the Kauzmann temperature, the liquid turns into a glassy solid, with a different, solid-like thermal expansion. In the case of prilocaine, this happens around 218–219 K. The difference between the specific volumes of the glassy solid and that of the crystalline solid (at 219 K) is 0.0653 cm $^3$  g $^{-1}$ ; the specific volume of the crystalline solid is smaller than that of the glass, as expected.

**3.4. Pressure–Temperature Melting Curve for Racemic Prilocaine.** HP-DTA experiments demonstrate that the temperature of fusion of racemic prilocaine increases as a function of pressure in the range of 0–250 MPa as can be seen in Figure 7. The data were fitted to ( $r^2 = 0.9992$ )

$$P/\text{MPa} = -1474(22) + 4.7(2)T/\text{K} \quad (3)$$

not changed after 20 years of storage, a strong indication that the prilocaine sample did not degrade. Quenching the melt resulted in a glass, and on reheating a glass transition was observed between 218 and 219 K (midpoint).

**3.3. Specific Volume as a Function of Temperature.** The specific volume of racemic prilocaine was measured in the solid and liquid phases. The results can be seen in Figure 6. The specific volume of molten racemic prilocaine was found to

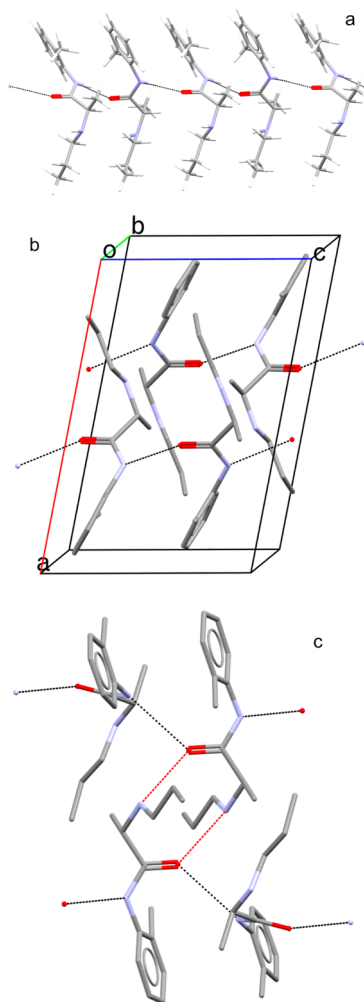


**Figure 5.** Details of the structure of Prilocaine. (a) Hydrogen-bond chain along the *c* axis with interchanging (R)- and (S)-prilocaine. (b) The infinite hydrogen-bond chain runs along the *c* axis of the unit cell. The rings and the aliphatic chains form planes parallel to *b*. (c) Weaker hydrogen-bond chains along the *b* axis form (R)-(S) dimers.

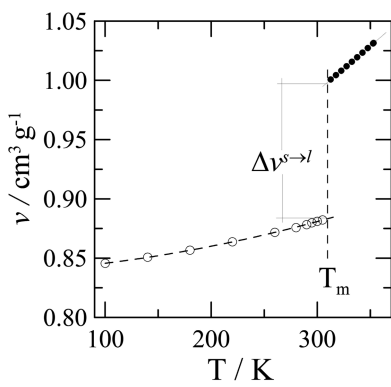


**Figure 6.** Specific volume of solid and liquid prilocaine as a function of temperature. The specific volume difference between the liquid and the solid state is indicated as  $\Delta v^{s \rightarrow l}$ .

The initial slope of the pressure–temperature curve can also be calculated with the Clapeyron equation:

$$(dp/dT)_{\text{fus}} = \Delta_{\text{fus}}s / \Delta_{\text{fus}}v = \Delta_{\text{fus}}h / (T_{\text{fus}} \Delta_{\text{fus}}v) \quad (4)$$

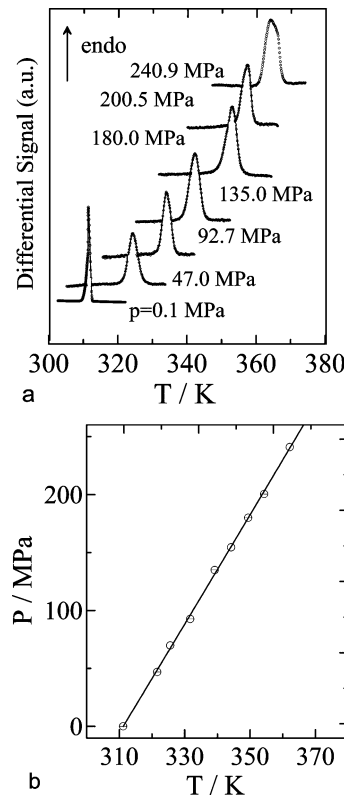


**Figure 7.** (a) Prilocaine melting curves measured by high-pressure differential thermal analysis. (b) Measurement pressure as a function of the measured prilocaine melting temperatures (peak onset).

$\Delta_{\text{fus}}s$  is the specific entropy change of fusion, and the other variables have been introduced above together with their values for prilocaine. They give rise to a value for the initial slope  $dP/dT$  at the melting point under ordinary conditions of  $4.1 \pm 0.4 \text{ MPa K}^{-1}$ , which is comparable to the slope of the linear fit to the direct measurements (eq 3).

**3.5. Demixing in the Binary System Prilocaine–Water.** DSC curves for the prilocaine–water system are presented in Figure 8. The temperature ( $T$ ) (onset, unless stated otherwise)

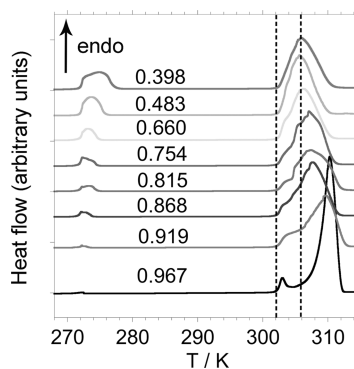


**Figure 8.** Typical DSC curves for prilocaine–water mixtures. The monotectic peak at 302.4 K can be observed for the 0.967 mol fraction. For the other mixtures down to 0.754 mol fraction the liquidus and the monotectic peaks have been convoluted. The last three peaks (0.660–0.398) represent the monotectic equilibrium underneath the miscibility gap. The peak at 273.1 K is the degenerate eutectic equilibrium between ice, prilocaine, and the saturated aqueous solution.

of the peaks has been plotted against the mole fraction ( $x$ ) in Figure 9a, and the enthalpy of the transition peaks has been

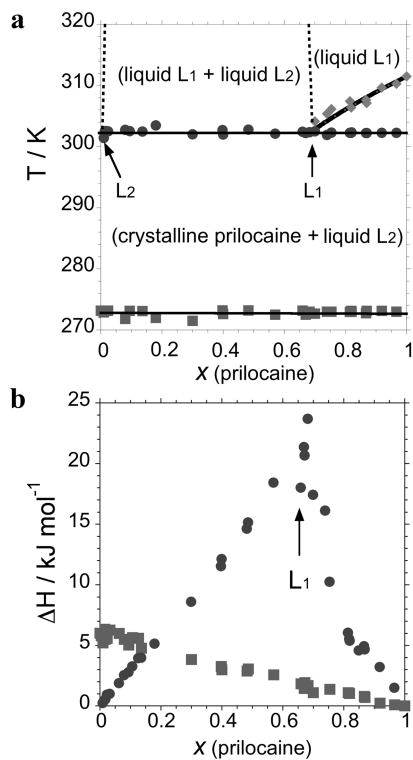


**Figure 9.** (a) Temperature–composition (mol fraction) phase diagram of the binary system prilocaine–water exhibiting a miscibility gap in the liquid phase.  $L_1$  is the prilocaine-rich liquid,  $L_2$  the water-rich liquid. Solid squares: eutectic equilibrium. Solid circles: monotectic equilibrium. Solid diamonds: liquidus related to the fusion of prilocaine. (b) Tammann plot (transition enthalpy change as a function of the mol fraction of the mixture) for the eutectic and monotectic equilibria.

plotted as a function of  $x$  in Figure 9b. At 273.1 K (0.0 °C), a peak can be observed increasing in enthalpy with increasing water concentration, indicating the presence of a degenerate eutectic equilibrium between three phases: pure solid water, a water-rich solution saturated with prilocaine, and pure solid prilocaine. The recorded temperature demonstrates that there is virtually no decrease in the melting temperature of solid prilocaine–ice mixtures with respect to the melting point of ice.

A second set of peaks can be found at 302.4 K (29.2 °C) (see Figure 8). They convolute very rapidly starting from the prilocaine-rich side. Analogous to the system of lidocaine–water,<sup>4</sup> the peaks at 302.4 K represent a monotectic equilibrium between two immiscible liquid phases and solid prilocaine. The liquids are a water-based solution saturated with prilocaine ( $L_2$ ) and a prilocaine-based solution saturated with water ( $L_1$ ) (see Figure 9). The demixing of the two liquids can be observed in Figure 10. The liquids remain stable for a minimum of two years at room temperature. Thus demixing even persists in the metastable domain below the temperature for the monotectic equilibrium as measured by DSC.

The interpretation of the peaks resulting from the monotectic equilibrium shift is aided by the  $T$ – $x$  phase diagram in Figure 9a. For pure prilocaine, fusion takes place at 311.5 K. Once water is added, the peak of fusion turns into a liquidus peak, which can be observed in the DSC curve of 0.967 mol fraction with a maximum at about 310 K (Figure 8). The small peak with an onset at 302.4 K belongs to the monotectic equilibrium. For lower concentrations of prilocaine, the monotectic peak and the liquidus peak are convoluted as mentioned above (Figure 8). This affects the precision of the determination of the concentration of  $L_1$  (prilocaine-rich liquid) by extrapolation of the Tammann plot (enthalpy change versus composition); the plot can be seen in Figure 9b. Nevertheless, the Tammann plot leads to an estimate for the concentration of  $L_1$  between 0.65 and 0.7 mol fraction.

To determine the concentration of  $L_1$ , it is also possible to use the maximum temperatures of the liquidus peaks, which can be extrapolated to the monotectic temperature with the Schröder equation; this leads to a composition for  $L_1$  between 0.69 and 0.67 mol fraction.

The value of 0.69 is the estimate for ideal behavior and is obtained from the data for prilocaine fusion (311.5 K and 147 J/g) by direct application of the Schröder equation; the resulting curve follows the liquidus values reasonably well and reaches 0.687 at the monotectic temperature of 302.4 K. As a verification, the first term of the Redlich–Kister expansion was added as a simple excess function to the Schröder equation:  $H_{\text{exc}}(1 - x)^2$ . The excess enthalpy term,  $H_{\text{exc}}$ , was optimized against the measured liquidus maxima using the least-squares method leading to a value of 582 J mol<sup>-1</sup>. This small value essentially indicates that the liquidus related to the fusion of prilocaine can be considered ideal between the melting point and the monotectic equilibrium. The Schröder equation with

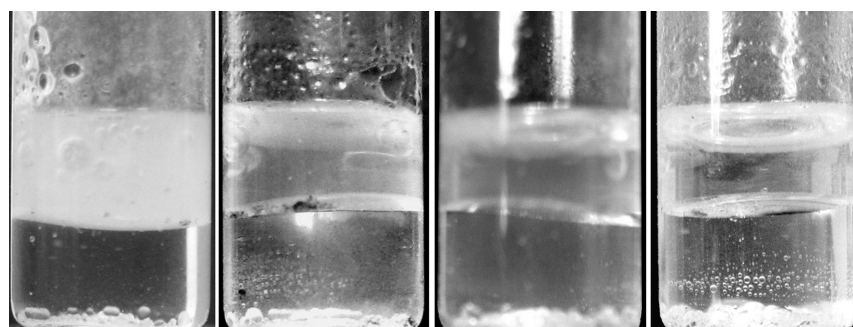


**Figure 10.** Evolution of the prilocaine–water system at room temperature. From left to right: 0, 8, 12, and 24 months after mixing. The liquid on top is oily and viscous in appearance and must therefore be the lidocaine-rich liquid (in addition, after two years this layer has turned slightly yellow). Its initial milky aspect is due to droplets of water-rich liquid that form a persistent emulsion “with no lipophilic solvent”, a clear indication that the densities of both liquids do not differ much.

the excess enthalpy leads to an intersection of the liquidus with the monotectic equilibrium at 0.669 mol fraction.

It can be observed that the three peaks at 302.4 K from 0.660 mol fraction downward (Figure 8) have the same onset and maximum, indicating that they represent the pure monotectic transition without any liquidus contribution resulting from the miscibility gap. It corroborates the concentration interval found for the monotectic equilibrium as the peak for 0.660 mol fraction must be located approximately at or just below the concentration of the prilocaine-rich liquid. The liquidus of the miscibility gap must increase quite rapidly with temperature, as no maximum critical temperature could be determined.

#### 4. DISCUSSION

The crystal structure clearly indicates that the studied prilocaine sample is a racemic compound and not a conglomerate, because both (*R*)- and (*S*)-prilocaine are present in the crystal structure. The two enantiomers alternate along an infinite hydrogen-bond chain along the *c* axis of the unit cell (Figure 5). Furthermore, a weaker hydrogen bond gives rise to (*R*)- and (*S*)-enantiomer pairs interconnecting the infinite hydrogen-bond chains.

The change of specific volume as a function of temperature of molten racemic prilocaine,  $d\nu/dT$ , is  $7.66 \times 10^{-4} \text{ cm}^3 \text{ g}^{-1} \text{ K}^{-1}$  ( $0.169 \text{ cm}^3 \text{ mol}^{-1} \text{ K}^{-1}$ , eq 1), which is smaller than the value  $9.33 \times 10^{-4} \text{ cm}^3 \text{ g}^{-1} \text{ K}^{-1}$  ( $0.219 \text{ cm}^3 \text{ mol}^{-1} \text{ K}^{-1}$ ) found for molten lidocaine.<sup>4</sup> This indicates that intermolecular interactions in molten prilocaine should be somewhat stronger than those in lidocaine. Ternidazole, a 2-methyl-5-nitroimidazole with antiprotozoal and antibiotic properties, has a liquid volume change with temperature of  $5.09 \times 10^{-4} \text{ cm}^3 \text{ g}^{-1} \text{ K}^{-1}$  (185.19 g/mol).<sup>26</sup> These three values lead to an average specific volume change with temperature in the liquid for these small organic molecules of  $7.36 \times 10^{-4} \text{ cm}^3 \text{ g}^{-1} \text{ K}^{-1}$ . This value is of importance for the estimation of thermal expansion in the liquid phase for APIs, if such data cannot be obtained experimentally, for example due to decomposition in the melt.

The *P-T* melting curve for prilocaine is almost straight in the pressure range of 0 to 250 MPa. In the case of lidocaine, the solid–liquid equilibrium is somewhat more curved. Their initial slopes are respectively 4.7 and 3.56 MPa K<sup>-1</sup>.<sup>4</sup> This indicates that, relatively speaking, pressure stabilizes the solid state in the case of lidocaine more than in the case of prilocaine and that the solid–liquid equilibrium of prilocaine is slightly less influenced by pressure with respect to temperature.

The volume changes on melting are about  $0.110 \pm 0.003 \text{ cm}^3 \text{ g}^{-1}$  ( $24.3 \text{ cm}^3 \text{ mol}^{-1}$ ) for prilocaine, twice as large as that of lidocaine with  $0.057 \text{ cm}^3 \text{ g}^{-1}$  ( $13.3 \text{ cm}^3 \text{ mol}^{-1}$ ).<sup>4</sup> A similar difference is found for the entropy changes on melting:  $99.3 \text{ J mol}^{-1} \text{ K}^{-1}$  for prilocaine and  $47.5 \text{ J mol}^{-1} \text{ K}^{-1}$  for lidocaine.<sup>4</sup> Prilocaine gains more in entropy and more in volume on melting. These data add some nuance to the analysis of the *P-T* melting curves above. Pressure favors large (negative) volume changes, which would favor the melting of prilocaine under pressure over the melting of lidocaine. However, the large entropy change of fusion of prilocaine is favored by the temperature, and in this case the increase of entropy offsets the large volume change of prilocaine on melting in comparison to the changes observed for lidocaine (see also eq 4, the Clapeyron equation). Under ordinary conditions, pressure is low for both prilocaine and lidocaine, therefore the lower melting temperature of prilocaine may be an immediate result of its higher entropy change on melting.

A monotectic equilibrium is present at 302.4 K in the prilocaine–water diagram; this implies the presence of a prilocaine-rich liquid, which can be considered as a solution of water in prilocaine. At the monotectic equilibrium composition, 0.3 mol of water dissolves in 0.7 mol of prilocaine (i.e.,  $\approx 966 \text{ mg prilocaine/mL solution}$ ). In comparison with the solubility of prilocaine in water at 302.04 K, 7.0 mg/mL,<sup>1</sup> it is obvious that the prilocaine-rich liquid L<sub>1</sub> will be a much more effective anesthetic than the saturated solution in water.

As stated in the Introduction, lidocaine–water mixtures exhibit a monotectic equilibrium at 321 K.<sup>4</sup> The lidocaine-rich liquid contains approximately 0.7 mol fraction in lidocaine like in the case of prilocaine. This is very high compared to the concentration in its saturated aqueous solution (at 302.4 K for comparison with prilocaine) of 3.7 mg/mL.<sup>1</sup> The monotectic equilibrium containing prilocaine and water is even below the temperature of the human epidermis, ensuring that the mixture will be liquid, when applied to the skin.

Both the lidocaine and prilocaine systems exhibit a monotectic equilibrium with water. It is likely that a mixture of the three constituents (lidocaine, prilocaine, and water) will result in a ternary monotectic equilibrium at a temperature that is even lower than the one found for the prilocaine water system. In that case, the two immiscible liquids in the ternary mixture, one rich in lidocaine and prilocaine and one rich in water, will remain in the liquid state at room temperature and form a “nonconventional” stable emulsion. The temperature of the monotectic equilibrium lies even below room temperature, which can be deduced from the lidocaine–prilocaine system, which contains a eutectic equilibrium at 293 K.<sup>1</sup> As the latter temperature effectively represents the “melting temperature” of the prilocaine–lidocaine mixture, it is only reasonable that the monotectic equilibrium with water should be at least a few degrees below the eutectic temperature. This conclusion is confirmed by the observations reported by Brodin and Nyqvist-Mayer et al.<sup>1-3</sup>

#### 5. CONCLUSION

Prilocaine does not degrade while stored at room temperature for 20 years in a hermetically closed container in the dark. Its vapor pressure is high enough to cause sublimation and recrystallization. The resulting crystalline powder has been used to obtain the crystal structure of prilocaine from high-resolution powder diffraction.

Physical properties of prilocaine have been determined, such as the melting properties and the expansion of the specific volume with temperature. The slope of the melting transition in the pressure–temperature phase diagram has been obtained by direct measurement and with the Clapeyron equation.

A comparison of the prilocaine–water system and the lidocaine–water system leads to the conclusion that the “emulsion system [that] does not contain any lipophilic solvent”<sup>3</sup> is in fact demixing of two liquids, one rich in prilocaine and lidocaine and one rich in water. The system remains stable, because the underlying monotectic equilibrium for the ternary system is most likely found below ambient temperature. This can be concluded, first, because the monotectic equilibria between water and either prilocaine or lidocaine are found well below their respective melting temperatures and, second, because the eutectic mixture of prilocaine and lidocaine possesses a eutectic temperature of 293 K.

## AUTHOR INFORMATION

### Corresponding Author

\*E-mail: ivo.rietveld@parisdescartes.fr. Tel: +33 1 53 73 96 75.

### Notes

The authors declare no competing financial interest.

## ACKNOWLEDGMENTS

We thank Jacco van de Streek and Marcus Neumann (Avant-Garde Materials Simulation, Freiburg, Germany) for the DFT calculations and discussion. M.B. and J.-L.T. were supported by the Spanish Ministry of Science and Innovation (Grant FIS2011-24439) and the Catalan Government (Grant 2009SGR-1251).

## REFERENCES

- (1) Brodin, A.; Nyqvist-Mayer, A.; Wadsten, T.; Forslund, B.; Broberg, F. Phase-Diagram and Aqueous Solubility of the Lidocaine Prilocaine Binary-System. *J. Pharm. Sci.* **1984**, *73* (4), 481–484.
- (2) Nyqvist-Mayer, A. A.; Brodin, A. F.; Frank, S. G. Phase Distribution Studies on an Oil-Water Emulsion Based on a Eutectic Mixture of Lidocaine and Prilocaine as the Dispersed Phase. *J. Pharm. Sci.* **1985**, *74* (11), 1192–1195.
- (3) Nyqvist-Mayer, A. A.; Brodin, A. F.; Frank, S. G. Drug Release Studies on an Oil-Water Emulsion Based on a Eutectic Mixture of Lidocaine and Prilocaine as the Dispersed Phase. *J. Pharm. Sci.* **1986**, *75* (4), 365–373.
- (4) Céolin, R.; Barrio, M.; Tamarit, J. L.; Veglio, N.; Perrin, M. A.; Espeau, P. Liquid-liquid Miscibility Gaps and Hydrate Formation in Drug-Water Binary Systems: Pressure-Temperature Phase Diagram of Lidocaine and Pressure-Temperature-Composition Phase Diagram of the Lidocaine-Water System. *J. Pharm. Sci.* **2010**, *99* (6), 2756–2765.
- (5) Fournival, J. L.; Rouland, J. C.; Céolin, R. Polymorphism of barbital and the barbital-water system. *J. Therm. Anal.* **1987**, *32* (5), 1547–1557.
- (6) Fournival, J. L.; Rouland, J. C.; Céolin, R. Phenobarbital-water system. *J. Therm. Anal.* **1988**, *34* (1), 161–175.
- (7) Ballon, J.; Comparat, V.; Pouxe, J. The blade chamber - A solution for the curved gaseous detectors. *Nucl. Instrum. Methods Phys. Res., Sect. A* **1983**, *217*, 213–216.
- (8) Evain, M.; Deniard, P.; Jouanneaux, A.; Brec, R. Potential of the Inel X-Ray Position-Sensitive Detector - a General Study of the Debye-Scherrer Setting. *J. Appl. Crystallogr.* **1993**, *26*, 563–569.
- (9) Rodriguez-Carvajal, J.; Roisnel, T.; Gonzales-Platas, J. *Full-Prof suite version 2005*; Laboratoire Léon Brillouin, CEA-CNRS, CEA Saclay: Saclay, France, 2005.
- (10) Neumann, M. A. X-Cell: a novel indexing algorithm for routine tasks and difficult cases. *J. Appl. Crystallogr.* **2003**, *36*, 356–365.
- (11) Engel, G. E.; Wilke, S.; Konig, O.; Harris, K. D. M.; Leusen, F. J. J. PowderSolve - a complete package for crystal structure solution from powder diffraction patterns. *J. Appl. Crystallogr.* **1999**, *32*, 1169–1179.
- (12) Hanson, A. W.; Banner, D. W. 2-Diethylamino-2',6'-Acetoxylidide (Lidocaine). *Acta Crystallogr., B* **1974**, *30* (Oct 15), 2486–2488.
- (13) Coelho, A. A. *TOPAS Academic version 4.1 (Computer Software)*; Coelho Software: Brisbane, 2007.
- (14) Dollase, W. A. Correction of Intensities for Preferred Orientation in Powder Diffractometry - Application of the March Model. *J. Appl. Crystallogr.* **1986**, *19*, 267–272.
- (15) Bruno, I. J.; Cole, J. C.; Kessler, M.; Jie, L.; Motherwell, W. D. S.; Purkis, L. H.; Smith, B. R.; Taylor, R.; Cooper, R. I.; Harris, S. E.; Orpen, A. G. Retrieval of crystallographically-derived molecular geometry information. *J. Chem. Inf. Comput. Sci.* **2004**, *44*, 2133–2144.
- (16) Neumann, M. A. *GRACE (Computer Software)*; see <http://www.avmatsim.eu>.
- (17) Kresse, G.; Furthmüller, J. Efficient iterative schemes for ab initio total-energy calculations using a plane-wave basis set. *Phys. Rev. B: Condens. Matter* **1996**, *54*, 11169–11186.
- (18) Kresse, G.; Hafner, J. Ab initio molecular dynamics for liquid metals. *Phys. Rev. B: Condens. Matter* **1993**, *47*, 558–561.
- (19) Kresse, G.; Joubert, D. From ultrasoft pseudopotentials to the projector augmented-wave method. *Phys. Rev. B: Condens. Matter* **1999**, *59*, 1758–1775.
- (20) Wang, Y.; Perdew, J. P. Correlation hole of the spin-polarized electron gas, with exact small-wave-vector and high-density scaling. *Phys. Rev. B: Condens. Matter* **1991**, *44*, 13298–13307.
- (21) Neumann, M. A.; Perrin, M.-A. Energy ranking of molecular crystals using density functional theory calculations and an empirical van der Waals correction. *J. Phys. Chem. B* **2005**, *109*, 15531–15541.
- (22) Van de Streek, J.; Neumann, M. A. Validation of experimental molecular crystal structures with dispersion-corrected density functional theory calculations. *Acta Crystallogr., B* **2010**, *66*, 544–558.
- (23) Deringer, V. L.; Hoepfner, V.; Dronskowski, R. Accurate Hydrogen Positions in Organic Crystals: Assessing a Quantum-Chemical Aide. *Cryst. Growth Des.* **2012**, *12* (2), 1014–1021.
- (24) Naelapaa, K.; van de Streek, J.; Rantanen, J.; Bond, A. D. Complementing high-throughput X-ray powder diffraction data with quantum-chemical calculations: Application to piroxicam form III. *J. Pharm. Sci.* **2012**, *101* (11), 4214–4219.
- (25) Würflinger, A. Differential thermal-analysis under high-pressure IV. Low-temperature DTA of solid-solid and solid-liquid transitions of several hydrocarbons up to 3 kbar. *Ber. Bunsen-Ges. Phys. Chem.* **1975**, *79* (12), 1195–1201.
- (26) Mahe, N.; Perrin, M.; Barrio, M.; Nicolai, B.; Rietveld, I.; Tamarit, J.; Ceolin, R. Solid-State Studies of the Triclinic ( $Z = 2$ ) Antiprotozoal Drug Ternidazole. *J. Pharm. Sci.* **2011**, *100* (6), 2258–2266.